Chemical Engineering Journal 160 (2010) 779–787

Contents lists available at ScienceDirect

Chemical Engineering Journal

journal homepage: www.elsevier.com/locate/cej

An injectable oxidized carboxymethylcellulose/N-succinyl-chitosan hydrogel system for protein delivery

Shaoyu Lü, Mingzhu Liu*, Boli Ni

State Key Laboratory of Applied Organic Chemistry, Key Laboratory of Nonferrous Metal Chemistry and Resources Utilization of Gansu Province and Department of Chemistry, Lanzhou University, Lanzhou 730000, People's Republic of China

ARTICLE INFO

Article history:
Received 22 December 2009
Received in revised form 18 March 2010
Accepted 29 March 2010

Keywords:
Injectable
Oxidized carboxymethylcellulose
N-succinyl-chitosan
Biodegradable
Protein delivery

ABSTRACT

This work is focused on the development of a new injectable drug delivery system for proteins sustained release. A series of in situ forming hydrogels derived from oxidized carboxymethylcellulose (OCMC) and N-succinyl-chitosan (NSC) were prepared by Schiff base reaction. OCMC was prepared by cleaving the vicinal glycols in carboxymethylcellulose with sodium periodate and NSC was obtained by introduction of succinyl groups into chitosan N-terminal of the glucosamine units, respectively. The gelation readily took place at physiological pH and temperature. Several parameters, such as matrix gelation time, equilibrium swelling ratio, matrix degradation rate and drug release profile, were investigated. The in vitro cytotoxicity studies showed that the OCMC/NSC hydrogels were non-cytotoxic and preserved the viability of the entrapped cells. The release profile of BSA was divided into four stages, indicating that the release of BSA was controlled by both diffusion and degradation. Importantly, activity of released BSA was retained regardless of the oxidation degree. This newly described OCMC/NSC hydrogels demonstrated attractive properties and would be a suitable injectable and biodegradable system for the delivery of protein drugs.

1. Introduction

During the past decade, the use of hydrogels as biomaterials has been the subject of ample research based on their potential application in drug delivery, especially for protein drug delivery [1–3]. The key for the generalized use of these systems depends on developing hydrogels with an adequate structure in terms of porosity and biological properties, such as hydrophilicity and biocompatibility. The porosity can tune the diffusion rate of the macromolecules and subsequently the protein release rate [4]. The hydrophilicity provides an aqueous environment for the delicate proteins to prevent them from denaturation. Hydrogels are generally considered biocompatible due to their physiochemical similarity to the macromolecular-based components in the body and minimally invasive administration to the body [5,6]. However, several challenges still remain, such as potential cytotoxicity of organic solvents and cross-linkers, instability of protein during preparation of hydrogels, and losing biological activity after administration into the body [7,8].

With these shortcomings in mind, in situ forming hydrogel based release systems for proteins are being developed. These systems are injectable fluids that can be introduced into the body in a minimally invasive manner prior to gelling within the desired tissue, organ, or body cavity [9]. Gelation can occur in situ due to the change in pH [10] or temperature [11], or by ionic cross-linking [12], which does not require initiators or cross-linkers. Protein drugs can be incorporated by simple pre-mixing. However, the in situ forming hydrogel systems for protein drugs delivery also present considerable challenges. The gelation conditions for in vivo use are limited to a narrow range of physiologically acceptable temperatures, and the cross-linking must occur with no byproducts in a sensitive aqueous environment [13]. Furthermore, gelation must occur at a sufficiently rapid rate avoiding a large amount of drugs diffusing away from the injection site and leading to drug overdosage, yet sufficiently slow that complete mixing occurs prior to gelation and avoiding clogging of the needle [13,14]. In addition, the release of proteins from hydrogels is generally diffusion-controlled, and the sustained release over a long time period may not be expected when the proteins are physically entrapped in the hydrogels [15]. For the in situ forming systems, biodegradability of hydrogels is also an important factor. The hydrogels can be broken down and then cleared by the body. Therefore, it eliminates the need for surgery to remove the device after the drug is released. Moreover, the release of the entrapped protein can be regulated by the degra-

* Corresponding author at: Department of Chemistry, Lanzhou University, Lanzhou 730000, People's Republic of China. Tel.: +86 931 8912387; fax: +86 931 8912582.
E-mail address: mzliu@lzu.edu.cn (M. Liu).

1385-8947/$ – see front matter © 2010 Elsevier B.V. All rights reserved.
doi:10.1016/j.cej.2010.03.072

dation behavior of the hydrogels, as well as by the simple diffusion [16].

Biomaterials such as oxidized cellulose and cellulose derivatives have been employed as injectable materials for biomedical applications based on their excellent biocompatibility and biodegradability [17]. Water-soluble chitosan derivative is another attractive base material for in situ cross-linkable matrices [18–20]. In the present study, carboxymethylcellulose (CMC) was partially oxidized with sodium periodate to form oxidized carboxymethylcellulose (OCMC) which was then cross-linked in situ with N-succinyl-chitosan (NSC) to form injectable hydrogels. OCMC and NSC cross-linked at physiological pH and temperature by electrostatic interaction, hydrogen bonding and eventually stabilization by Schiff base formation between aldehyde and amine groups located on the two molecules. Schiff's bonds are susceptible to hydrolytic cleavage in aqueous conditions. Therefore, these bonds in the cross-linked OCMC/NSC hydrogels should provide a degradable linkage. The release of a model protein drug, bovine serum albumin (BSA), from these hydrogels was monitored in vitro and the activity of BSA released from the hydrogels was examined to assess the suitability of OCMC/NSC hydrogel as a protein delivery device.

2. Materials and methods

2.1. Materials

The sodium salt of carboxymethylcellulose (CMC, MW 250,000, carboxymethylation degree of 0.91 per disaccharide unit) was supplied by Wealthy Chemical Industry Co., Ltd. (Suzhou, China). Chitosan (CS, MW 270,000, deacetylation degree of 90.8%) was obtained from Golden-Shell Biochemical Co., Ltd. (Zhejiang, China). Succinic anhydride, sodium periodate, ninhydrin and other chemicals were analytical grade and used as received.

2.2. Synthesis of oxidized carboxymethylcellulose (OCMC)

Different amounts of sodium periodate (in aqueous solution) was added to a CMC aqueous solution (1% (w/v), 100 ml) and stirred at ambient temperature for 2 h in the dark to obtain OCMC with different degree of oxidation. An equimolar of diethylene glycol was added to quench any unreacted periodate. The mixture was stirred for 1 h and then dialyzed exhaustively for 3 days against water and pure OCMC was obtained by lyophilization. The oxidation degree of OCMC was defined as the percentage of CMC structure units that have been oxidized, and it was determined by measuring the number of aldehyde groups in partially oxidized carboxymethylcellulose. Excess amount of *tert*-butyl carbazates was added to the polymer solution and reacted with the aldehydes to form stable carbazones. The amount of unreacted *tert*-butyl carbazates was determined by adding the solution of trinitrobenzenesulfonic acid (TNBS). The absorbance of the colored complex of *tert*-butyl carbazates and TNBS was measured at 334 nm using a UV/vis spectrophotometer (Lambda 35, PerkinElmer, America). Values reported for the oxidation degree were average of three oxidation experiments.

2.3. Synthesis of N-succinyl-chitosan (NSC)

NSC was prepared according to a previous reported procedure slightly modified [19]. Briefly, 1 g of chitosan was dissolved in 60 ml 5% (v/v) lactic acid solution and then 60 ml of methanol was added to dilute the solution. Afterwards, 3 g of succinic anhydride was added at room temperature while stirring. The reaction was continued for total of 24 h, and the products were collected and precipitated by adding 500 ml of KOH-ethanol solution. The precipitation was filtered, re-dissolved in water, dialyzed for 3 days, and lyophilized. The substitution degree of NSC was determined by the ninhydrin assay. 1 g of ninhydrin was dissolved in 100 ml of glycerol/water (1:2, v/v) solution and the resulting solution was stored in a dark bottle. To 1 ml of NSC aqueous solution, 1 ml of 2 M sodium acetate buffer (pH 5.5) and 1 ml of the ninhydrin reagent were added in sequence. The tube was immediately capped, shaken, and heated in a boiling water bath for 10 min, and then cooled to room temperature. The content was diluted with 7 ml of 60% (v/v) ethanol/water solution for absorbance measurement at 570 nm using a UV/vis spectrophotometer. Values reported for the substitution degree were average of three experiments.

2.4. Characterization by size exclusion chromatography (SEC)

Polymer molecular weights were characterized by size exclusion chromatography (SEC) using a Waters Alliance GPCV2000 (USA) equipped with three detectors on line: a differential refractometer, a viscometric detector and a multiangle laser light scattering (MALLS) detector from Wyatt (USA). Aqueous sodium nitrate (0.1 M) at ambient temperature with nominal flow rate of 0.5 ml/min was used as the mobile phase. Weight-average molar mass (Mw) was obtained as characteristic of the polymers.

2.5. Formation of OCMC/NSC hydrogels

Solution of 30 mg/ml of OCMC and NSC were prepared separately in 10 ml of phosphate buffered saline (PBS, pH 7.4, 0.1 M). Then equal volumes (200 μl) of each polymer solution were mixed at room temperature to obtain cross-linked hydrogels. The gelation time of the resulting hydrogels was measured using a previously described method [21]. The solution of OCMC and NSC were mixed with a magnetic stir bar on a petri dish at 155 rpm using a stirrer. The gelation time was the time until the mixture became a globule and values reported were average of five determinations.

2.6. Characterization of OCMC/NSC hydrogels

2.6.1. Fourier transform infrared spectroscopy

Fourier transform infrared (FTIR) spectroscopy was carried out with Nicolet NEXUS 670 FTIR spectrometer. The samples were dried completely and ground to fine power, then push down to piece blending with KBr.

2.6.2. Scanning electron microscopy

The porous structure of the hydrogels was examined by scanning electron microscopy (SEM). The hydrogels were prepared and freeze-dried using a LABCONCO Freeze Dryer. The dried samples were fractured, coated with gold and the microstructures and morphologies of the cross-sections of the hydrogels were then examined by a JSM-5600LV SEM (Japan) with an operating voltage of 20 kV.

2.7. Swelling behavior of OCMC/NSC hydrogels

The equilibrium swelling ratio (*ESR*) of the hydrogels was measured in PBS at 37 °C. Preweighed dry samples were immersed in PBS solution until they swelled to equilibrium. After excess surface water was removed with filter paper, the fully swollen samples were weighed. All experiments were done in triplicate. The *ESR* can be calculated by Eq. (1):

$$ESR = \frac{W_e - W_d}{W_d} \quad (1)$$

where W_e and W_d are the weights of equilibrium hydrated gel and dry gel, respectively.

The water diffusion coefficient (D) was calculated by Eq. (2):

$$\frac{M_t}{M_\infty} = 1 - \sum_{n=0}^{\infty} \frac{8}{(2n+1)^2\pi^2} \exp\left\{\frac{-D(2n+1)^2\pi^2 t}{\delta^2}\right\} \quad (2)$$

The early-time approximation of Eq. (2) can be written as Eq. (3) [22]:

$$\frac{M_t}{M_\infty} = 4\left(\frac{Dt}{\pi\delta^2}\right)^{0.5} \quad (3)$$

where δ is the initial thickness of the flat gel sheet, M_t and M_∞ are the mass of water absorbed at time t and at equilibrium, respectively.

2.8. Degradation studies

In order to study the degradability of the hydrogels, in vitro degradation tests were carried out in PBS at 37 °C. The degradation process was monitored by measuring the dry weight loss. Each hydrogel was placed in a vessel containing 50 ml of PBS. At predetermined time intervals, hydrogels were moved from the PBS solution and then dried under vacuum at room temperature to constant weight. All experiments were done in triplicate. The weight loss ratio (WLR) was calculated by Eq. (4):

$$WLR\ (\%) = \frac{W_0 - W_t}{W_0} \times 100 \quad (4)$$

where W_0 and W_t are the weights of hydrogels before and after degradation, respectively.

2.9. Cytotoxicity test

Cytotoxicity evaluation of hydrogels was performed by 3-[4,5-dimethylthiazol-2-yl]-2,5-diphenyl tetrazolium bromide (MTT) assay using HEK 293T cells, which were grown in DMEM with 10% of fetal bovine serum (FBS) and were cultured in a humidified atmosphere containing 5% CO_2 at 37 °C. Solution of 30 mg/ml of OCMC and NSC were sterilized by autoclave, respectively. Equal volumes (20 μl) of the OCMC and NSC solution were injected into a 96-well plate, mixed, and incubated at 37 °C to form hydrogels. Then 200 μl of culture medium containing 1×10^4 cells was added into each well. This was left at 37 °C for 24 h. Then, the medium was replaced by fresh DMEM. After 48 h, the cell cultures were washed with PBS solution and MTT assay was conducted. Untreated cells were taken as control with 100% viability. The cell cytotoxicity of hydrogels was defined as the relative viability (%) which correlates with amount of liable cells compared with cell control. Reported values were mean of three replicates.

2.10. In vitro protein release studies

To study the release behavior of the protein, OCMC/NSC hydrogels loaded with 83 mg/g of BSA were prepared. BSA was mixed with 200 μl of NSC solution to form a homogenous solution, then 200 μl of OCMC solution with different oxidation degree was added and the mixture was vortexed gently. Round gel disks with diameter of 1.2 cm were formed using a circular mold. Each disk was dried under vacuum at room temperature to constant weight and then placed in 50 ml of PBS solution at 37 °C. At fixed time intervals, 5 ml of the release medium was withdrawn and replaced immediately with fresh buffer. The protein content was determined using UV/vis spectroscopy at 280 nm. All experiments were done in triplicate. The amount of BSA released at time t (M_i) was calculated by Eq. (5):

$$M_i = 50 \times C_i + 5 \times \sum C_{i-1} \quad (5)$$

where C_i is the concentration of BSA in the release medium at time t.

The percentage of BSA released (PR, %) at each interval was calculated using Eq. (6):

$$PR\ (\%) = \frac{M_i}{M_\infty} \times 100 \quad (6)$$

where M_∞ is the total loaded BSA in the hydrogels.

2.11. Activity of BSA released from OCMC/NSC hydrogels

Hydrogels loaded with 83 mg/g of BSA were immersed in 50 ml of PBS at 37 °C. At predetermined time intervals, the activity of the BSA released into the release medium was determined using a fluorescence spectrophotometer (LS 55, PerkinElmer, America). The synchronous fluorescence spectra of BSA were recorded from 200 to 400 nm at $\Delta\lambda = 60$ nm. The activity retained was determined by comparing to the maximum emission wavelength of control protein solution which was freshly prepared. Values reported were average of three experiments.

2.12. Statistical analysis

Statistical analysis of data was performed by one-way analysis of variance (ANOVA), assuming confidence level of 95% ($p < 0.05$) for statistical significance. All data were expressed as mean ± standard deviation (S.D.).

3. Results and discussion

3.1. Characterization of OCMC/NSC in situ forming hydrogels

Periodate oxidation specifically cleaves the vicinal glycols in polysaccharide to form their dialdehyde derivatives that could serve as a macromolecular cross-linker for those polymers bearing free amino groups to form hydrogels [23,24]. In this study, OCMC was obtained by oxidizing CMC with sodium periodate (Scheme 1a). The oxidation degree was controlled by the mole equivalent of sodium periodate used in each reaction and estimated by measuring the number of aldehydes in the final products. As summarized in Table 1, the actual oxidation degrees of OCMC with theoretical oxidation degrees of 20.0%, 40.0%, 60.0% and 80.0%, were determined as 17.4 ± 0.4%, 36.6 ± 0.4%, 55.2 ± 0.3% and 74.5 ± 0.4%, respectively. As expected, the oxidation degree of OCMC increased as the amount of added periodate was increased (Table 1). Determination of the Mw of OCMC showed significant depolymerization of CMC (Table 1), which was due to increase in the extent of oxidation and associated polymer cleavage.

NSC was obtained by introduction of succinyl groups into chitosan N-terminal of the glucosamine units (Scheme 1b). The molecular weight of NSC was determined to be 231,900 ± 9230. Ninhydrin reacted with a primary amine group to form a colored reaction product [25]. The substitution degree was evaluated by determining the remaining unreacted primary amino groups in NSC and it was 48.1 ± 0.3%. The content of free amine groups of the succinyl chitosan was 28.6 ± 0.9%. The ratio of amine groups and aldehyde groups was shown in Table 2.

Hydrogels was formed by cross-linking OCMC with NSC (Scheme 1c). The formation of hydrogels was predominantly due to Schiff base reaction between the aldehyde groups of OCMC and the amino groups of NSC. One attractive feature of this system is that gelation occurs without requiring additional initiators, cross-linkers or light sources. Furthermore, gelation time can be tuned by altering the oxidation degree of OCMC. It has been reported that

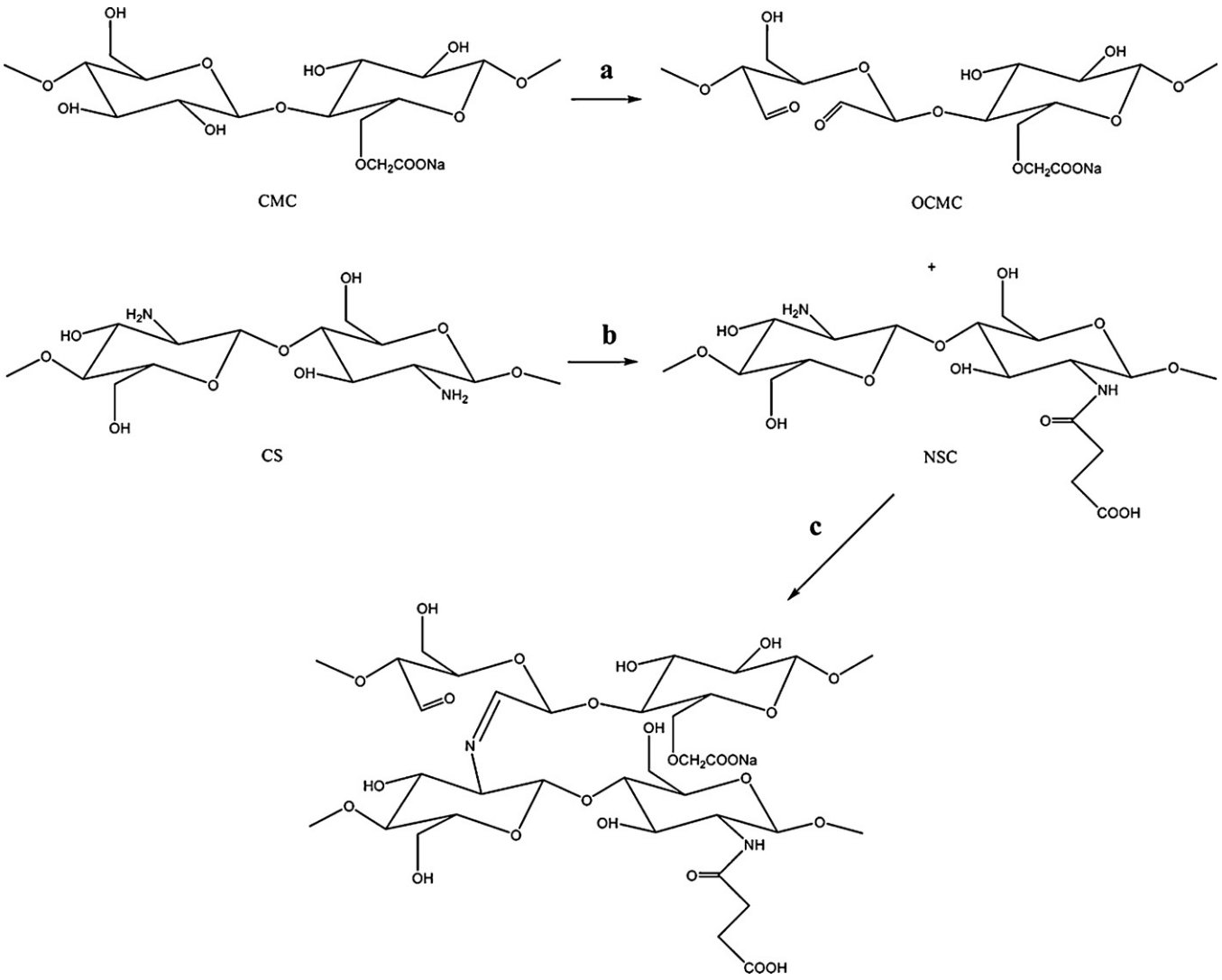

Scheme 1. Synthetic route of (a) OCMC, (b) NSC, and (c) OCMC/NSC hydrogel.

Table 1
Degree of oxidation, aldehyde content and M_w of the products obtained by oxidizing carboxymethylcellulose with sodium periodate.

Sample	Periodate equivalent (%)	Degree of oxidation (%)	Aldehyde content (%)	M_w (g/mol)
OCMC-1	20.0	17.4 ± 0.4	14.4 ± 0.3	213,100 ± 8520
OCMC-2	40.0	36.6 ± 0.4	30.2 ± 0.3	73,930 ± 3690
OCMC-3	60.0	55.2 ± 0.3	45.6 ± 0.2	43,300 ± 2160
OCMC-4	80.0	74.5 ± 0.4	61.5 ± 0.3	32,230 ± 1620

the gelation time is crucial because slow gelation would cause delocalized gel formation due to diffusion of the gel precursors away from the injection site, while fast gelation would clog the needle before injection [14]. The gelation time was determined at room temperature and the results are shown in Table 2. It is noted that gelation occurs in a reasonably short time (47 ± 5 to 178 ± 9 s). In addition, the higher the oxidation degree of OCMC is, the faster the gelation rate. It is because that more aldehyde groups presented and facilitated the gel formation with higher oxidation degree of OCMC.

3.1.1. FTIR analysis

Fig. 1 shows the FTIR spectra of polysaccharide derivatives and OCMC/NSC hydrogels. A peak at 1735 cm^{-1} (aldehyde symmet-

Table 2
Summary of results of the gelling properties of OCMC/NSC hydrogels.

Sample	Amine groups:aldehyde groups	Gelling time (s)	Average pore diameter (μm)	Equilibrium swelling ratio	Water diffusion coefficient ($\times 10^4$ mm^2/s)
Gel-1	1:0.5	178 ± 9	29.6 ± 5.6	87.7 ± 3.8	6.84 ± 1.81
Gel-2	1:1.1	103 ± 8	26.9 ± 4.7	57.9 ± 1.7	3.00 ± 0.37
Gel-3	1:1.6	60 ± 2	22.1 ± 4.0	33.7 ± 2.1	1.32 ± 0.72
Gel-4	1:2.2	47 ± 5	13.9 ± 2.7	24.1 ± 1.4	0.96 ± 0.56

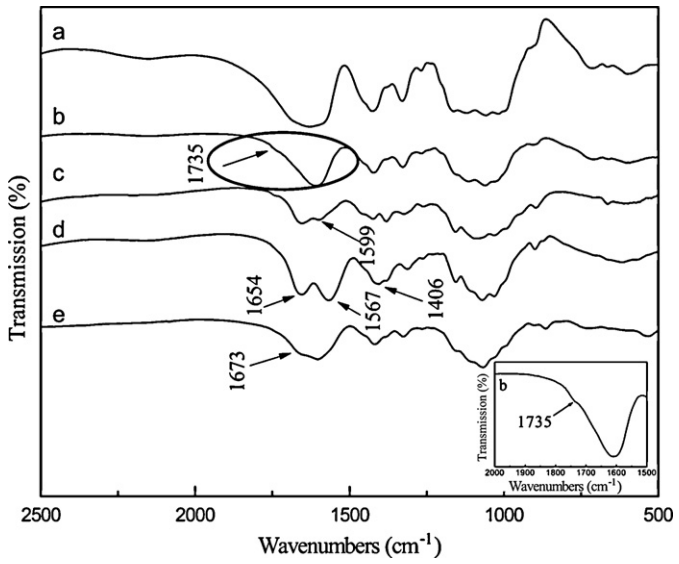

Fig. 1. FTIR spectra of CMC (a), OCMC (b), CS (c), NSC (d) and OCMC/NSC hydrogel (e). The inset shows the magnification of the spectrum of OCMC (b) from 1500 to 2000 cm^{-1}.

ric vibration) is detected in the spectrum of OCMC (Fig. 1b and the inset), compared with that of CMC (Fig. 1a). It is unconspicuous and this may be due to the hemiacetal formation of free aldehyde groups [26]. A characteristic peak at 1599 cm^{-1} in CS spectrum (Fig. 1c) can be ascribed as $-NH_2$ bending vibration. In the spectrum of NSC (Fig. 1d), it is noted that the band at 1599 cm^{-1} decreases while a new prominent band at 1567 cm^{-1} (–NH– bending vibration) appears and the bands at 1654 cm^{-1} (Amide I) and 1406 cm^{-1} (Amide III) become broader, indicating the substitution of the CS. Similar observation has been reported by other researchers in the succinyl chitosan [27,28]. In the spectrum of the hydrogel (Fig. 1e), the characteristic band of the Schiff base structure (–C=N–) at 1673 cm^{-1} suggests that the coupling reaction was occurred between –CHO of OCMC and $-NH_2$ of NSC.

3.1.2. SEM observations

The scanning electron micrographs of hydrogels are shown in Fig. 2. The hydrogels exhibit a continuous and porous structure. These structural properties of the matrices may be responsible for offering a larger specific surface area, and therefore, a better matrix-solvent interaction, allowing easier solvent uptake and drug diffusion. Pore size analysis gives a pore diameter in the range of 10–35 μm (Table 2). It is found that pore size distribution changed with change in composition of the hydrogels. Fig. 2b–d shows the smaller three-dimensional net-hole with increasing the oxidation degree of OCMC. It is because of the higher cross-linking density with larger oxidation degree of OCMC. Therefore, it can be inferred that the swelling extent of hydrogels will be smaller with a higher oxidation degree of OCMC.

3.2. Swelling behavior

Hydrogels was formed by cross-linking OCMC with NSC. The characteristics of the hydrogel can be modulated by varying the oxidation degree of OCMC in the composition of the feed mixture. Swelling behavior of OCMC/NSC hydrogels in PBS at 37 °C as a function of time is shown in Fig. 3. As can be seen, all the

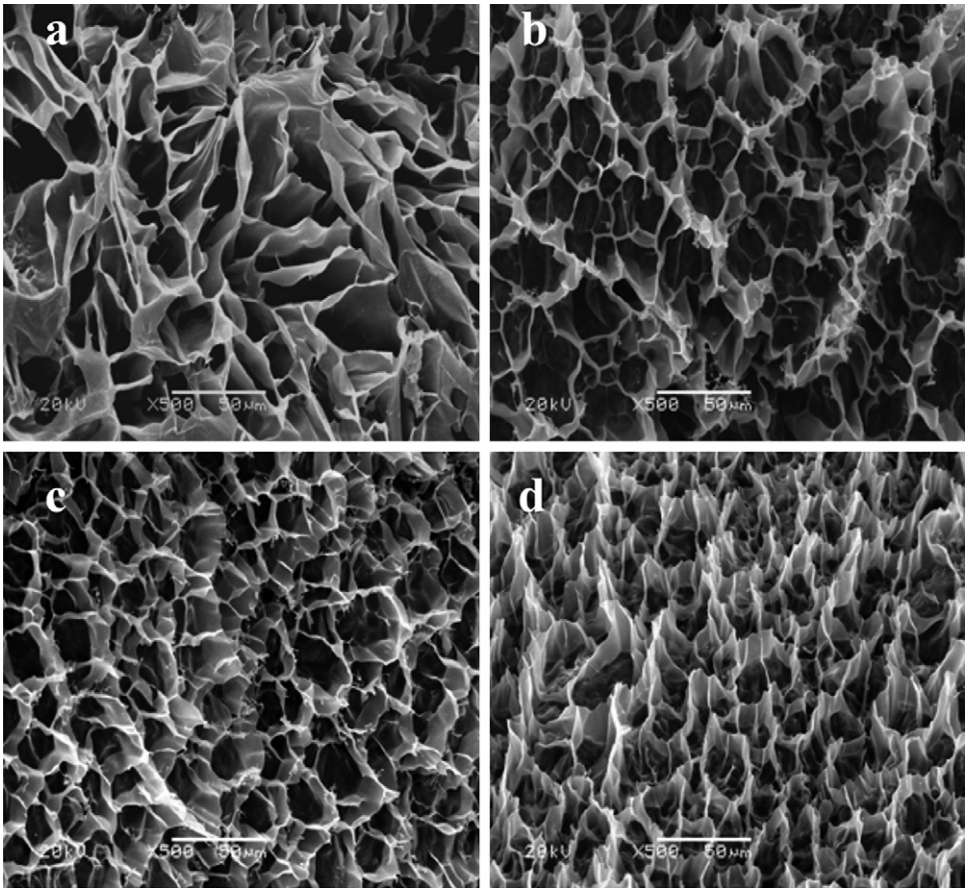

Fig. 2. SEM images of the hydrogels. (a) Gel-1; (b) Gel-2; (c) Gel-3; (d) Gel-4.

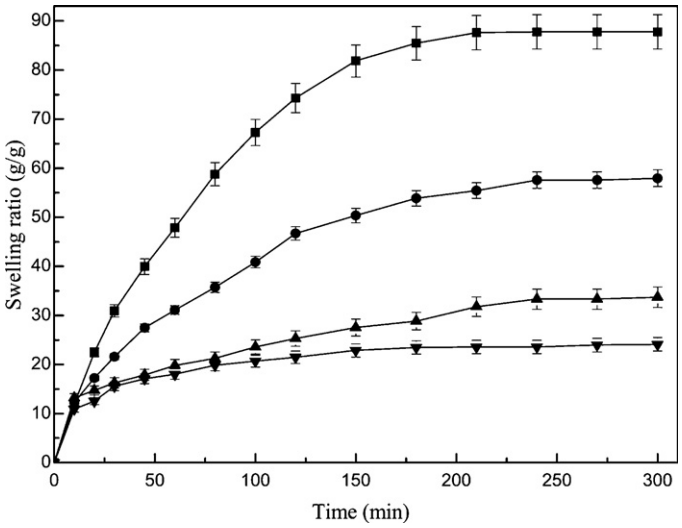

Fig. 3. Swelling behavior of OCMC/NSC hydrogels in PBS at 37 °C as a function of time. (■) Gel-1; (●) Gel-2; (▲) Gel-3; (▼) Gel-4.

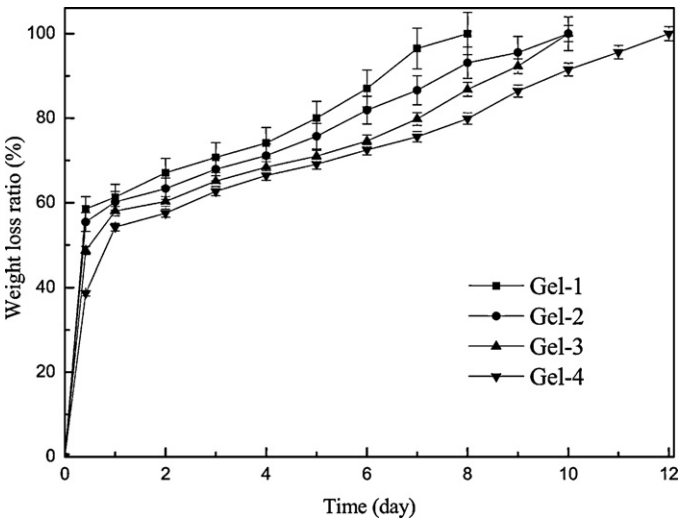

Fig. 4. Weight loss ratio of OCMC/NSC hydrogels in PBS at 37 °C as a function of time.

hydrogels have high swelling ratio, because both OCMC and NSC have a large number of hydrophilic groups, such as hydroxyl, carboxyl and amino groups, which obviously result in an enhanced water uptake and consequently a large swelling ratio. Table 2 shows the equilibrium swelling ratio (*ESR*) and water diffusion coefficient (*D*) of the hydrogels. The *ESR* decreases with the oxidation degree of OCMC increasing, which is in agreement with the foregoing SEM results. As the oxidation degree of OCMC increases, the number of aldehyde groups available for cross-linking also increases, which consequently causes the formation of compact networks and decreases the *ESR* of the hydrogels. Obviously, *D* increases with *ESR* increasing. Also, the case that *D* increases with an increase in the pore size is observed (Table 2), indicating that the water diffusion coefficient has a close connection with the gel microstructure. When the pore size is small, the migration of water molecules in the gel network as well as the relaxation of the polymer segment is difficult, resulting in a lower value of *D*. When the pore size is large enough, the polymer segment is expanded, therefore, the ingress and diffusion of water molecules would be easy and the value of *D* would be higher, i.e. the case for Gel-1 and Gel-2.

3.3. Degradation

The degradability of the hydrogels was monitored by examining the weight loss of hydrogels with incubation time in PBS at 37 °C, as shown in Fig. 4. A decrease in weight with time demonstrates the degradability of the hydrogels. It has been shown that the type of the degradable link and the structure of the network play an important role in the control of the degradation behavior [29]. In this study, the connectivity of the OCMC/NSC hydrogel network is maintained by the cross-linking of –CHO and $–NH_2$, which yield Schiff's linkage. Therefore, degradation of the hydrogels is due to the hydrolytic susceptibility of Schiff's linkage. After incubation in PBS for 24 h, the weight loss ratio is 61.3 ± 3.1%, 60.2 ± 2.5%, 58.0 ± 1.1% and 54.2 ± 0.9% for Gel-1, Gel-2, Gel-3 and Gel-4, respectively. The results indicate that Schiff base cross-linking structure is instable, which was also reported by Ito et al. [21]. The degradation process can be described as follows: initially, a small number of Schiff bonds are broken, which cannot damage the whole hydrogel network, but the lattice size of the networks will enlarge, resulting in a large swelling ratio (data not shown). Then, the breakage of the Schiff bonds reaches a critical value and the whole cross-linking network will be disjointed, resulting in disintegration of the hydrogels.

The degradation is related to the oxidation degree of OCMC, as shown in Fig. 4. When the oxidation degree of OCMC increases, the resulting hydrogels show strong ability against degradation. It is understandable that a higher oxidation degree of OCMC will form more aldehyde groups, and then yield a higher cross-linking degree. This is confirmed by the fact that the swelling ratio of Gel-4 (24.1 ± 1.4 times) in PBS at 37 °C is much smaller than that of the Gel-1 (87.7 ± 3.8 times). The higher cross-linking density consequently decreases the exposure of polymer chains to water molecules, leading to smaller weight loss.

3.4. Cytotoxicity

It is known that the cytotoxicity of the biomaterials is extremely important for their future applications. To evaluate the present hydrogels as a potential delivery system for biomacromolecules, the cytotoxicity of the prepared hydrogels was investigated by MTT assay. The influence of the hydrogels on the proliferation of HEK 293T cells was examined and displayed in Fig. 5. The results demon-

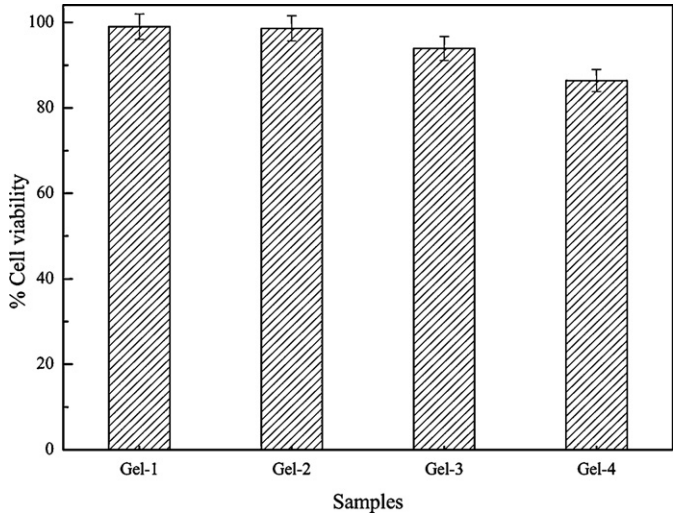

Fig. 5. Cell viability measured by MTT assay for different samples after 48 h of incubation.

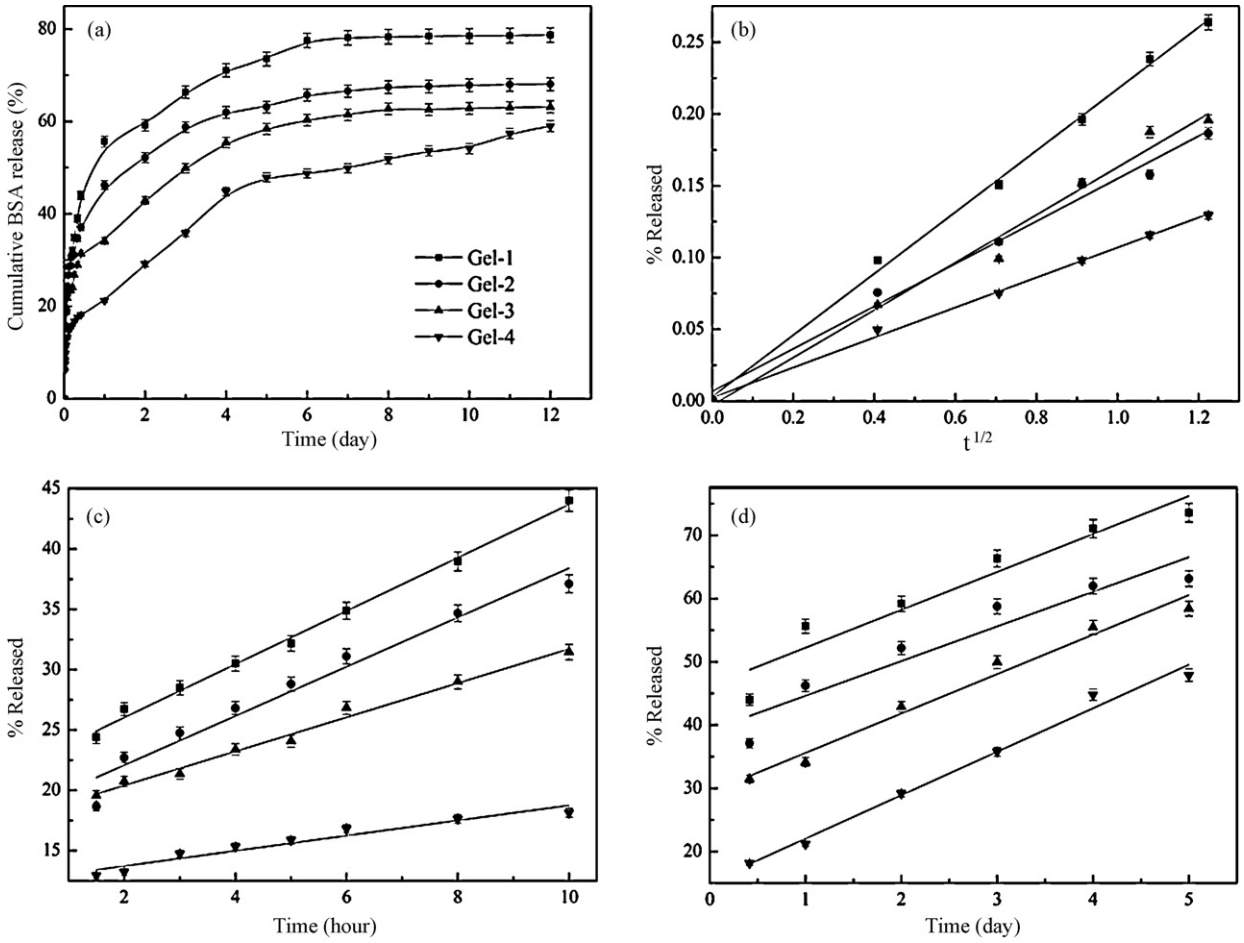

Fig. 6. Release profiles of BSA from hydrogels in PBS at 37 °C. (a) Cumulative BSA released from hydrogels in 12 days; (b) BSA released from 0 to 90 min; (c) BSA released from 90 min to 10 h; (d) BSA released from 10 h to 5 days.

strate that, after 48 h, the cells are more than 93% viable in the testing concentration in relation to the control for Gel-1, Gel-2 and Gel-3, indicating that any of the hydrogels has no apparent cytotoxicity. However, the viability for Gel-4 decreases to 86.4 ± 2.6%, showing that the higher oxidation degree affects cell viability.

3.5. Drug release

The model protein BSA was used for the release experiment and the release kinetics in PBS at 37 °C are depicted in Fig. 6. The aim here was to investigate whether the release of the entrapped protein can be regulated by the degradation of the hydrogels, as well as by the simple diffusion.

In a system, where drug is entrapped in a biodegradable matrix, the release rate depends on three parameters: the size of the drug molecule, the cross-linking density and the degradation rate [29]. The hydrodynamic diameter of BSA is 7.2 nm [30], which is less than the mesh sizes of OCMC/NSC hydrogels (Table 2), suggesting that the protein could diffuse freely within the network and the release was predicted to be largely due to diffusion. Indeed, by plotting the release of BSA during the first 90 min as a function of the square root of time, a linear plot is obtained, indicating the release is Fickian diffusion (Fig. 6b). It is found that swelling is fast during the first 90 min (Fig. 3). It can be expected that the permeation of BSA through the matrix will increase with an increase in the swelling level of the matrix. Therefore, in the first 90 min, diffusion is fast as compared to degradation and no effect of polymer degradation on release can be expected. A first-order profile is observed for all hydrogels. In the subsequent stage of release (90 min to 10 h), an almost constant release rate is observed (Fig. 6c), indicating the release is a virtually constant zero-order rate. This suggests that the drug may diffuse out of the system in parallel with the degradation of the hydrogels. This argument can be fully justified when comparing the release kinetics (Fig. 6a) with the weight loss profile (Fig. 4). In the first 10 h, the BSA released from the hydrogels is 44.0 ± 0.8%, 37.1 ± 0.7%, 31.5 ± 0.6% and 18.1 ± 0.4% for Gel-1, Gel-2, Gel-3 and Gel-4, respectively. In the same time, the weight loss ratio of the hydrogels is 58.5 ± 3.0%, 55.4 ± 2.3%, 48.7 ± 0.9% and 38.7 ± 0.6%, respectively. It is reported that the decline in release rate caused by the reduced drug concentration in the matrix may be compensated by an increase of the diffusion coefficient due to polymer degradation, to yield an almost constant release rate [7]. This concept of drug diffusion enhanced by polymer degradation can be used to explain the zero-order profile of BSA released from OCMC/NSC matrices from 90 min to 10 h. In the third stage of release (10 h to 5 days), near zero-order kinetics are also found (Fig. 6d), indicating that the release of BSA is dominated by diffusion together with degradation. The release rate becomes smaller compared to the second stage, because the degradation rate from 10 h to 5 days is slower than that from 90 min to 10 h. At the last stage, the release behavior comes to a moderate stage when most of the free BSA is released. Therefore, it is inferred that the release of the macromolecular model drug BSA is dominated by diffusion together with degradation, rather than by a diffusion mechanism.

From Fig. 6a, release of BSA from Gel-1 is fast as compared to release from the other matrices. The effect of the composition on

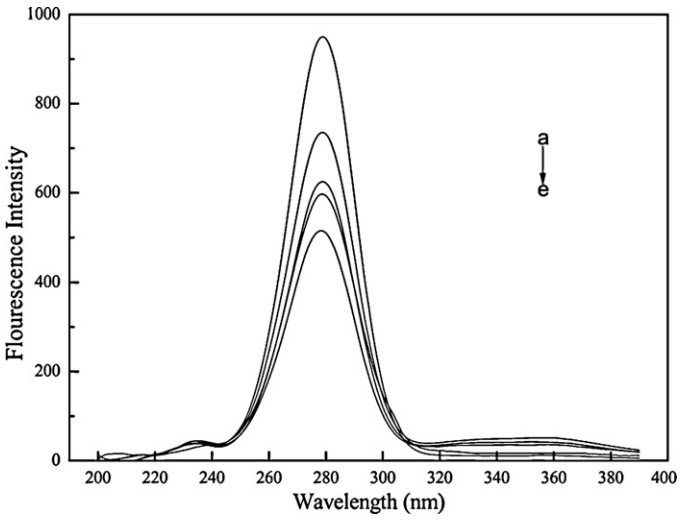

Fig. 7. Synchronous fluorescence spectra of BSA at $\Delta\lambda = 60$ nm. (a) BSA freshly prepared; (b) BSA released from Gel-1 after 12 days; (c) BSA released from Gel-2 after 12 days; (d) BSA released from Gel-3 after 12 days; (e) BSA released from Gel-4 after 12 days.

the release rate can be explained by the difference in degree of cross-linking. The cross-linking density increases, as we illustrated before, resulting in the average molecular distance between adjacent cross-linking point reducing and hence the diffusivity of drugs in the hydrogel decreases. On the contrary, lower cross-linking density results in initially looser contact and an increase in gel pore size, making more protein release. However, even in the case of the hydrogel based on the lowest cross-linking density (Gel-1), not all BSA is completely released within 12 days. The remaining part may be entrapped in the hydrogels as the amino functions of BSA can enter into Schiff's reaction with the aldehyde groups of OCMC.

3.6. Activity of released BSA from OCMC/NSC hydrogels

It is important that a protein release system not only delivers the proteins at a controlled release rate but also maintains the activity of the proteins. Protein denaturation may occur during formulation, storage, and release periods. It has been reported that degraded products of polylactides and copolymers generate a pH drop within the polymer matrices, which may cause loss of biological activity of the protein [8,31]. It may excepted that OCMC/NSC system will cause less protein stability problems due to the non-toxicity of the hydrogels and since the degraded products generate less acid end-groups in time.

It has been reported that fluorescence emission is much more sensitive to changes in the environment of the chromophore than its light absorption, thus fluorescence spectroscopy is an excellent method to investigate conformational changes of proteins [32–34]. In this study, synchronous fluorescence spectra gained at $\Delta\lambda = 60$ nm are used to analyze the change of the conformation of BSA, as shown in Fig. 7. When $\Delta\lambda = 60$ nm, the synchronous fluorescence spectra exhibits the spectral character of tryptophan residues. The maximum emission wavelength of tryptophan residues is related to the polarity of the environment and the change of emission wavelength is thus used to estimate that of protein conformation.

It can be seen from Fig. 7 that the maximum emission wavelength of tryptophan residue keeps unchanged even after BSA released for 12 days, which shows that there is no significant change in the conformation of the released BSA, indicating that this protein is not damaged during the formulation, storage and release periods. This result suggests that the OCMC/NSC hydrogel is a suitable injectable and biodegradable system for the delivery of therapeutic proteins.

4. Conclusions

A in situ forming and biodegradable hydrogel system was achieved from carboxymethylcellulose and chitosan without incorporating any extraneous cross-linking agents. The gelation time, equilibrium swelling and degradation can be modulated by adjusting the oxidation degree of carboxymethylcellulose. The OCMC/NSC hydrogels with a higher oxidation degree showed a shorter gelation time and a lower equilibrium swelling and degradation rate than those of hydrogels with a lower oxidation degree. The results of in vitro cytotoxicity studies demonstrated that the hydrogels showed good cell viability and are non-cytotoxic. Sustained release of BSA was observed through both diffusion-controlled and degradation-controlled mechanism. Activity of released BSA remained regardless of the oxidation degree. These studies indicate that the OCMC/NSC in situ forming hydrogel may have potential uses in protein drugs delivery.

Acknowledgement

The authors gratefully acknowledge the financial support of the Special Doctorial Program Fund of the Ministry of Education of China (Grant No. 20090211110004) and Gansu Province Project of Science and Technologies (Grant No. 0804WCGA130).

References

[1] A.S. Hoffman, Hydrogels for biomedical applications, Adv. Drug Del. Rev. 54 (2002) 3–12.
[2] N. Bhattarai, H.R. Ramay, J. Gunn, F.A. Matsen, M. Zhang, PEG-grafted chitosan as an injectable thermosensitive hydrogel for sustained protein release, J. Control. Release 103 (2005) 609–624.
[3] J.B. Leach, C.E. Schmidt, Characterization of protein release from photocrosslinkable hyaluronic acid-polyethylene glycol hydrogel tissue engineering scaffolds, Biomaterials 26 (2005) 125–135.
[4] D.-Q. Wu, F. Qiu, T. Wang, X.-J. Jiang, X.-Z. Zhang, R.-X. Zhuo, Toward the development of partially biodegradable and injectable thermoresponsive hydrogels for potential biomedical applications, Appl. Mater. Interfaces 1 (2009) 319–327.
[5] Y.H. Bae, S.W. Kim, Hydrogel delivery systems based on polymer blends, block co-polymers or interpenetrating networks, Adv, Drug Deliv. Rev. 11 (1993) 109–135.
[6] K.Y. Lee, D.J. Mooney, Hydrogels for tissue engineering, Chem. Rev. 101 (2001) 1869–1880.
[7] J.M. Bezemer, R. Radersma, D.W. Grijpma, P.J. Dijkstra, J. Feijen, C.A. van Blitterswijk, Zero-order release of lysozyme from poly(ethylene glycol)/poly(butylene terephthalate) matrices, J. Control. Release 64 (2000) 179–192.
[8] T.G. Park, W. Lu, G. Crotts, Importance of in vitro experimental conditions on protein release kinetics, stability and polymer degradation in protein encapsulated poly (-lactic acid-co-glycolic acid) microspheres, J. Control. Release 33 (1995) 211–222.
[9] E. Ruel-Gariépy, J.-C. Leroux, In situ-forming hydrogels—review of temperature-sensitive systems, Eur. J. Pharm. Biopharm. 58 (2004) 409–426.
[10] Y.-L. Chiu, S.-C. Chen, C.-J. Su, C.-W. Hsiao, Y.-M. Chen, H.-L. Chen, H.-W. Sung, pH-triggered injectable hydrogels prepared from aqueous N-palmitoyl chitosan: in vitro characteristics and in vivo biocompatibility, Biomaterials 30 (2009) 4877–4888.
[11] K.M. Park, S.Y. Lee, Y.K. Joung, J.S. Na, M.C. Lee, K.D. Park, Thermosensitive chitosan-Pluronic hydrogel as an injectable cell delivery carrier for cartilage regeneration, Acta Biomater. 5 (2009) 1956–1965.
[12] A. Rozier, C. Mazuel, J. Grove, B. Plazonnet, Gelrite®: a novel, ion-activated, in-situ gelling polymer for ophthalmic vehicles. Effect on bioavailability of timolol, Int. J. Pharm. 57 (1989) 163–168.
[13] X. Zheng Shu, Y. Liu, F.S. Palumbo, Y. Luo, G.D. Prestwich, In situ crosslinkable hyaluronan hydrogels for tissue engineering, Biomaterials 25 (2004) 1339–1348.
[14] F. Lee, J.E. Chung, M. Kurisawa, An injectable hyaluronic acid-tyramine hydrogel system for protein delivery, J. Control. Release 134 (2009) 186–193.
[15] K.Y. Lee, S.H. Yuk, Polymeric protein delivery systems, Prog. Polym. Sci. 32 (2007) 669–697.
[16] B. Jeong, Y.H. Bae, D.S. Lee, S.W. Kim, Biodegradable block copolymers as injectable drug-delivery systems, Nature 388 (1997) 860–862.

[17] T. Ito, Y. Yeo, C.B. Highley, E. Bellas, D.S. Kohane, Dextran-based in situ cross-linked injectable hydrogels to prevent peritoneal adhesions, Biomaterials 28 (2007) 3418–3426.
[18] C.A. Falabella, M.M. Melendez, L. Weng, W. Chen, Novel macromolecular crosslinking hydrogel to reduce intra-abdominal adhesions, J. Surg. Res. 159 (2010) 772–778.
[19] H. Tan, C.R. Chu, K.A. Payne, K.G. Marra, Injectable in situ forming biodegradable chitosan-hyaluronic acid based hydrogels for cartilage tissue engineering, Biomaterials 30 (2009) 2499–2506.
[20] L. Weng, X. Chen, W. Chen, Rheological characterization of in situ crosslinkable hydrogels formulated from oxidized dextran and N-carboxyethyl chitosan, Biomacromolecules 8 (2007) 1109–1115.
[21] T. Ito, Y. Yeo, C.B. Highley, E. Bellas, C.A. Benitez, D.S. Kohane, The prevention of peritoneal adhesions by in situ cross-linking hydrogels of hyaluronic acid and cellulose derivatives, Biomaterials 28 (2007) 975–983.
[22] C.S. Brazel, N.A. Peppas, Mechanisms of solute and drug transport in relaxing, swellable, hydrophilic glassy polymers, Polymer 40 (1999) 3383–3398.
[23] W.E Hennink, C.F. van Nostrum, Novel crosslinking methods to design hydrogels, Adv. Drug Deliv. Rev. 54 (2002) 13–36.
[24] B. Balakrishnan, A. Jayakrishnan, Self-cross-linking biopolymers as injectable in situ forming biodegradable scaffolds, Biomaterials 26 (2005) 3941–3951.
[25] S. Prochazkova, K.M. Vårum, K. Ostgaard, Quantitative determination of chitosans by ninhydrin, Carbohydr. Polym. 38 (1999) 115–122.
[26] H.-A. Kang, G.-J. Jeon, M.-Y. Lee, J.-W. Yang, Effectiveness test of alginate-derived polymeric surfactants, J. Chem. Technol. Biotechnol. 77 (2002) 205–210.
[27] A. Zhu, T. Chen, L. Yuan, H. Wu, P. Lu, Synthesis and characterization of N-succinyl-chitosan and its self-assembly of nanospheres, Carbohydr. Polym. 66 (2006) 274–279.
[28] W. Sui, Y. Wang, S. Dong, Y. Chen, Preparation and properties of an amphiphilic derivative of succinyl-chitosan, Colloids Surf. Physicochem. Eng. Aspects 316 (2008) 171–175.
[29] A. Kelner, E.H. Schacht, Tailor-made polymers for local drug delivery: release of macromolecular model drugs from biodegradable hydrogels based on poly(ethylene oxide), J. Control. Release 101 (2005) 13–20.
[30] J.M. Bezemer, D.W. Grijpma, P.J. Dijkstra, C.A. van Blitterswijk, J. Feijen, A controlled release system for proteins based on poly(ether ester) block-copolymers: polymer network characterization, J. Control. Release 62 (1999) 393–405.
[31] R.E. Johnson, L.A. Lanaski, V. Gupta, M.J. Griffin, H.T. Gaud, T.E. Needham, H. Zia, Stability of atriopeptin III in poly(D,L-lactide-co-glycolide) microspheres, J. Control. Release 17 (1991) 61–67.
[32] N. Wang, L. Ye, F. Yan, R. Xu, Spectroscopic studies on the interaction of azelnidipine with bovine serum albumin, Int. J. Pharm. 351 (2008) 55–60.
[33] Y. Zheng, J. Lu, L. Liu, D. Zhao, J. Ni, Fluorescence analysis of aldolase dissociation from the N-terminal of the cytoplasmic domain of band 3 induced by lanthanide, Biochem. Biophys. Res. Commun. 303 (2003) 433–439.
[34] M. Gümüşderelioğlu, D. Kesgin, Release kinetics of bovine serum albumin from pH-sensitive poly(vinyl ether) based hydrogels, Int. J. Pharm. 288 (2005) 273–279.